RESEARCH ON MACHINING CENTER SPINDLE BEARING FAULT DIAGNOSIS BASED ON PARD-BP ALGORITHM

Dongmei LV[1], [2*], Xiaolei SUN[1], Zhang CHENG[1]

Combining working principle and failure mechanism of the three-main-shaft precision drilling and milling vertical machining center, analyzing the dynamical model of machining center spindle bearing, illustrating its failure phenomenon of the key components---the main shaft bearing, which will directly affect the performance of the power for the machining center. In order to make machining center spindle box work reliably, introducing PARD-BP neural network fault diagnosis algorithm, regarding machining center spindle box key components related fault samples data as input, and regarding fault mode matrix as target output. The diagnostic results of PARD-BP network are completely consistent with the test results. It can be seen from the analysis that PARD-BP network can identify mechanical faults and accurately diagnose faults. It is proved that PARD-BP algorithm is reliable for mechanical fault detection and diagnosis of spindle bearing.

Keywords: three-main-shaft machining center; Spindle system; PARD-BP Algorithm; Fault diagnosis; Network structure model

1. Introduction

With the wide application of electronic, sensor and computer technology in machinery industry, the technology of mechanical fault diagnosis develops rapidly. The system may completely or partially lose its function when it fails [1-3]. The traditional fault diagnosis technique is not very effective when analyzing the deep fault of the key parts of machining center with complex mechanical structure[4]. By integrating the knowledge of human logic thinking and image thinking into the diagnosis process, the deep and predictive fault diagnosis can be realized in real time and reliably.

XI et al.[5] studied fault diagnosis by establishing machine tool spindle bearing dynamic model. Berredjem et al. [6] studied the automatic induction of fuzzy rules from numerical data with the method of similarity division. CHENG et al. [7] studied the fault diagnosis of variable speed bearings based on [4] the fault characteristic coefficient template. In addition, Bayesian networks and decision trees have many applications in fault diagnosis. ZHANG et al. [8] conducted

[1] Anhui Communications Vocational and Technical College, Hefei 230051, China

[2] Institute of Mechanical and Automotive Engineering, Hefei University of Technology, Hefei 230009, China *Corresponding author: 362545768@qq.com

bearing fault diagnosis based on naive Bayes and decision tree by enhancing data independence. ZHOU et al. [9] used Bayesian networks to establish intelligent fault diagnosis and fault reasoning methods. ZHANG et al. [10,11] applied gradient lifting decision tree to data analysis of bearing fault diagnosis. Two kinds of data sets and time-frequency graph were constructed by using time series sorting transformation and continuous wavelet transform.

Based on the learning and training of Yolov5 algorithm, two kinds of machine vision models of pressure and velocity nephogram were obtained, and combined with statistical analysis, the preliminary diagnosis of impeller fault was realized. The way of improving the accuracy of impeller fault diagnosis is that two detection models were integrated based on the idea of stack integration [12]. The NPR-AFO method was introduced into mechanical fault diagnosis and compared with other existing decomposition methods through simulation and analysis of local fault data of rolling bearing. The proposed method can not only extract fault features effectively [13,14], but also state fault features are more obvious.

According to the typical fault diagnosis of the spindle bearings of the three-spindle precision drilling and tapping vertical machining center -- angular contact ball bearing, PARD-BP neural network model was established. In this paper, vibration signals of spindle and spindle bearing in x/y/z direction are comprehensively analyzed in the fault diagnosis of headstock, and the results of vibration diagnosis are fused [13,14]. After the vibration signals in all directions are diagnosed by PARD-BP neural network, the vibration information diagnosis is fused.

2. Main shaft bearing fault phenomena

The object studied in this paper is the physical object and coordinate system of the spindle system of the three-spindle precision drilling and tapping vertical machining center, as shown in Fig.1.The paper adds a physical picture of the spindle box of the machining center, from which it can be seen that +Z is vertical up, +X is horizontal left, and +Y is vertical to the paper (X-Z plane) according to the right-handed Cartesian coordinate system, pointing to the reader (operator).The detailed diagram of the spindle system of the research object in this paper is shown in Fig.2. From the perspective of components, spindle bearing faults mainly include inner ring fault (fatigue, fracture), outer ring fault (fatigue, fracture), rolling body fault (wear, fatigue), cage fault and other faults. According to statistics, 90% of the rolling bearing failure from the outer ring and inner ring failure [13-15], the main fault phenomena of gear include tooth surface wear and tooth surface contact fatigue, bending fatigue [16], broken teeth, tooth surface bonding and abrasion peeling, common wear mainly abrasive wear, corrosion wear, adhesive wear and tooth end impact wear, and related plastic deformation.

Fig.1 Spindle system of three spindle drilling-tapping vertical machining center

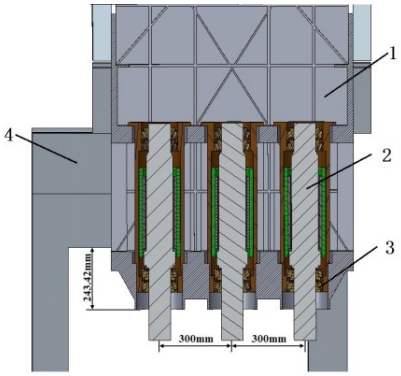

1-Spindle seat; 2-Spindle; 3-Spindle bearing; 4-Beam construction.

Fig.2 The machining centemain shaft system

Bearing fault diagnosis Algorithm method is similar to PARD-BP neural network fault diagnosis technology [16]. Self-Constructing algorithms are a widely used pruning technology in BP networks. Based on mathematical statistics, they introduce correlation coefficients and scatter in constructing and constructing hidden nodes to achieve constructing and merging control [12]. However, experimental data showed that when constructing Self-Constructing pruning methods, poor convergence, namely, the difficulty of constructing hidden-layer nodes into minimalism, was found. Therefore, the concept of randomness was introduced in constructing and constructing the pruning algorithm (PARD-BP), constructing and constructing the randomness algorithm in an integrated way. The

application of this algorithm in the fault diagnosis of spindle system in three-spindle precision drilling and tapping vertical machining center proves that the algorithm can effectively cut the hidden layer nodes of BP neural network to a minimum. In terms of diagnosis accuracy and network training time, PARD-BP neural network fault diagnosis technology with extremely condensed hidden layer nodes has obvious advantages compared with ordinary BP neural network.

3. PARD-BP neural network

3.1 Pruning Algorithm based on Random Degree (PARD-BP) algorithm

The self-configuration pruning algorithm with randomness RD is called PARD-BP algorithm. When randomness is zero, the PARD-BP algorithm degenerates into a general constructing Self-Constructing algorithm.

The idea of PARD-BP algorithm is shown in Figure 2, which comes from three aspects:

(1) The constructing possibility of Self-Constructing algorithms in itself is constructing consistent network structures.

(2) Transforming the disadvantages of randomness in initial weights and bias values into advantageous conditions in constructing convergent and consistent network structures in Self-Constructing algorithms. In essence, it is the application of probabilistic statistics techniques in constructing and constructing the concept of randomness.

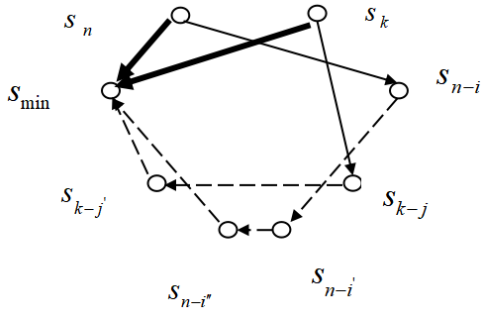

Fig. 3 Thought diagram of PARD-BP algorithm

(3) From the idea of divide-and-conquer algorithm, it is simply one task, that is, converging to a consistent network structure. When one step cannot be effectively completed or it is difficult to complete, each sub-task is completed in multiple steps, that is, pruning to a network structure first, starting with the network structure, continue pruning, and finally combine the sub-tasks, that is, the whole process of network pruning. To complete the whole task, that is, to achieve convergence of the network structure.

In Fig.3, h_n, h_k for a given number of hidden nodes (in which redundant nodes exist), the bold solid lines show that, when built in equal numbers, ideal Self-Constructing algorithms are able to shear from different numbers of hidden nodes to constructing a uniform, and the network structure has $h_{\min}$ hidden layer nodes. In fact, Self-Constructing algorithms (expressed in fine solid lines) can only h_n construct network structures in pruning which are constructed with h_{n-i} hidden layers of nodes, by stripping away i hidden nodes. After h_k pruning, a hidden layer with h_{k-j} network structure of nodes is formed. In generally, it is also demonstrated that Self-Constructing algorithms do not converge from constructing networks with different constructing node numbers in hidden layers to constructing networks with $h_{\min}$ individual constructing nodes. In PARD-BP (represented by dotted lines), the concept of randomness is utilized to repeatedly apply Self-Constructing algorithms in constructing or constructing networks of random initial weights. From h_{n-i}, h_{k-j} meridian $h_{n-i'}$, $h_{n-i''}$ or $h_{n-j'}$ the number of hidden layer node network structure, finally converges to or near it.

3.2 Normalization of feature parameters of PARD-BP algorithm

In the process of vibration signal acquisition, it will undoubtedly be affected by external factors, usually the noise pollution is very serious. The collected data will be analyzed and converted in the amplitude range so that the impact on vibration signals can be reduced [7-8]. The characteristic parameters are simple amplitude parameter extreme value, peak extreme value, root mean square value and dimensionless amplitude parameter [5]. Dimensionless amplitude parameters include waveform index, Extreme index and pulse index.

The signals of the normal operation and failure of the headstock are collected, and 8 types of common faults are selected [1]: inner ring fatigue, inner ring fracture, outer ring fatigue, outer ring fracture, rolling body wear, rolling body fatigue, cage failure. The calculation methods of each parameter are respectively.

Extreme value: $$E_{\max} = \max（E）\tag{1}$$

Peak-extreme value : $$E_{\text{pe}} = E_{\max} - E_{\min}\tag{2}$$

Root mean square value: $$E_{\text{rms}} = \left| \frac{1}{N} \sum_{i=1}^{N} \sqrt{|E_i|} \right|^2\tag{3}$$

Waveform index: $$W_{\text{f}} = E_i / \left| \bar{E}_i \right|\tag{4}$$

In the formula, $\bar{E}$ is Mean Value;

Extreme index: $$K_{\text{f}} = E_{\max} / E_{\text{rms}}\tag{5}$$

Pulse index: $C_{\mathrm{f}} = E_{\max} \Big/ \left|\bar{E}\right|$ (6)

The original data as characteristic parameters have different amplitudes, and sometimes the difference is quite large. If the neural network is directly input, when the measurement value fluctuates greatly, the learning process of neural networks will be affected, and it is difficult to reflect the change of small measurement value [14]. In order to classify and recognize various states by neural networks, it is necessary to remove the interference of physical units of each characteristic parameter, analyze only from the numerical value, and normalize between [0,1]. Therefore, the original data is normalized.

Common normalization processing methods are:

(1) Range normalization method:

$$e_i^{\,0} = \frac{e_i - e_{\min}}{e_{\max} - e_{\min}} \tag{7}$$

In the formula, $e_{\max} = \max\{e_i\}, e_{\min} = \min\{e_i\}$.

(2) Standard deviation normalization method:

$$e_i^{\,0} = \frac{e_i - \bar{e}}{\sigma} \tag{8}$$

In the formula, $\bar{e} = \frac{1}{n}\sum_{i=1}^{n} e_i$, $\sigma = \sqrt{\frac{1}{n-1}\sum_{i=1}^{n}(e_i - \bar{e})^2}$

(3)Mean normalization method:

$$e_i^{\,0} = \frac{e_i}{\bar{e}} \tag{9}$$

In the formula, $\bar{e} = \frac{1}{n}\sum_{i=1}^{n} e_i$.

The results obtained by the three data normalization processing methods are the same, but the range normalization method is the simplest [8]. Therefore, the range normalization method of Equation (1) is adopted to process the data, so that the normalized value falls between [0,1].

4. Headstock PARD-BP algorithm implementation

As an experimental device, Jiangsu Donghua DH5922N dynamic signal test analyzer collects signal dates and analyzes the dates. Bration signals of spindle bearing during normal operation, inner ring fatigue, inner ring fracture, outer ring fatigue, outer ring fracture, rolling body wear, rolling body fatigue and cage failure were collected. Vibration data network extraction training was carried out in

horizontal-direction, radial-direction and axial-direction [17]. Feature extraction was carried out on 6 groups of data extracted from each fault. Each group of data collected 150 points, and then the feature signal training processing, the obtained data into the neural network [18]. The fault warning table of normal operation (F0), inner ring fatigue (F1), inner ring fracture (F2), outer ring fatigue (F3), outer ring fracture (F4), rolling body wear (F5), rolling body fatigue (F6) and cage failure (F7) in the three directions of horizontal-direction, radial-direction and axial-direction were constructed. The fault mode symptom table of all directions is listed here, as shown in Tab.1, and the fault mode table of the above states is shown in Tab. 2.

To verify the validity of fault diagnosis for spindle bearing of machining center headstock, PARD-BP algorithm was introduced to simplify the network structure. To diagnose spindle bearings effectively, the working principle and fault diagnosis mechanism are analyzed according to the working characteristics of the spindle bearing, the data acquisition system of the spindle bearing is designed and implemented, and the monitoring equipment and parameters are described.

Table.1

Axial/Z-direction failure symptom table of key components

Failure mode Parameter	$E_{\max}$	E_{ff}	E_{rms}	W_{f}	K_{f}	C_{f}
Normal operation	0.4268	0.6379	0.6176	0.4376	0.6248	0.6324
Inner ring fatigue	0.4218	0.3978	0.3724	0.3365	0.4425	0.4097
Inner ring fracture	0.3364	0.3962	0.6200	0.6148	0.3136	0.3003
Outer ring fatigu	0.4476	0.3811	0.6049	0.6031	0.4137	0.4468
Outer ring fracture	0.4233	0.6011	0.4701	0.4424	0.3663	0.4473
Rolling wear	0.4420	0.4133	0.3263	0.2716	0.4182	0.4467
Rolling body fatigue	0.4137	0.5477	0.4476	0.4497	0.4135	0.4683
Cage failure	0.4578	0.4438	0.3876	0.6087	0.6561	0.4583

Table 2

Failure modes Table

State / Failure mode	F1	F2	F3	F4	F5	F6	F7
Normal operation	0	0	0	0	0	0	0
Inner ring fatigue	1	0	0	0	0	0	0
Inner ring fracture	0	1	0	0	0	0	0
Outer ring fatigue	0	0	1	0	0	0	0
Outer ring fracture	0	0	0	1	0	0	0
Rolling wear	0	0	0	0	1	0	0
Rolling body fatigue	0	0	0	0	0	1	0
Cage failure	0	0	0	0	0	0	1

In summary, the PARD-BP neural network for main shaft bearing fault diagnosis is reliable and effective. The adoption of PARD-BP genetic algorithm based on the algorithm is superior to the ordinary genetic algorithm [18] in terms of its consistent network structure convergence characteristics, simplified pruning property and its implication for the selection of randomness events. The BP algorithm is trained by

inputting fault sample data of axial piston pump and outputting fault mode target matrix.

Its output target matrix is

$$\mathrm{a}^2 = \text{logsig}\ （LW^2 * (\text{logsig}\ （IW^1 P + \mathrm{b}^1)) + \mathrm{b}^2）\tag{10}$$

In the formula:

$$W^1 = \begin{bmatrix} w_{1,1}^1 & w_{1,2}^1 & .... & w_{1,8}^1 \\ w_{2,1}^1 & w_{2,2}^1 & ... & w_{2,8}^1 \\ ... & ... & ... & ... \\ w_{k,1}^1 & w_{k,2}^1 & ... & w_{k,8}^1 \end{bmatrix} \quad b^1 = \begin{bmatrix} b_1^1 \\ b_2^1 \\ ... \\ b_k^1 \end{bmatrix}$$

$$W^2 = \begin{bmatrix} w_{1,1}^1 & w_{1,2}^1 & .... & w_{1,k}^1 \\ w_{2,1}^1 & w_{2,2}^1 & ... & w_{2,k}^1 \\ ... & ... & ... & ... \\ w_{7,1}^1 & w_{7,2}^1 & ... & w_{7,k}^1 \end{bmatrix} \quad b^2 = \begin{bmatrix} b_1^2 \\ b_2^2 \\ ... \\ b_7^{21} \end{bmatrix}$$

Combined with the working principle and fault mechanism of the three-spindle machining center, the possible fault cases were collected, and the working principle [1] and fault phenomena of the key spindle component of the three-spindle machining center -- rolling bearing were studied. The fault will directly affect the working performance of the spindle. In order to make the three-spindle machining center work reliably, the PARD-BP neural network fault diagnosis algorithm was introduced. PARD-BP algorithm takes spindle bearing vibration sample data as input and fault mode matrix as target output [19]. The results show that the PARD-BP algorithm is reliable for the fault detection and diagnosis of the main shaft bearing.

The establishment of spindle bearing fault diagnosis model based on genetic algorithm includes genetic algorithm optimization calculation and spindle bearing fault integral numerical simulation. Genetic algorithm can be used for the fault diagnosis and optimization of main shaft bearings. Compared with other traditional algorithms, it does not require derivatives or other auxiliary information, and only approximates the optimal solution by imitating the successful evolutionary process of genetic screening in nature [1].

PARD-BP network was used to detect the main shaft bearing fault sample data, and the horizontal direction vibration signal of the fault sample collected in history was normalized. Bearing fault sample data show in Tab. 3.

Table. 3

Fault sample data (horizontal-direction)

Inner ring fatigue (Sample 1)	0.3124	0.3067	0.4764	0.4261	0.4203	0.3844	0.3642	0.4643
Inner ring fracture (Sample 2)	0.3084	0.2901	0.4198	0.4119	0.3089	0.3064	0.2924	0.6809
Outer ring fatigue (Sample 3)	0.2279	0.2668	0.2443	0.2296	0.3402	0.2819	0.2644	0.6375
Outer ring fracture (Sample 4)	0.4291	0.4627	0.4864	0.4683	0.3102	0.4463	0.4784	0.3447

The structural parameters of the horizontal-direction vibration neural network after training[1] are shown in the Tab.4. After pruning, the number of hidden layer nodes of the object is reduced from 18 to 5.

Table 4

Reduction of axial /Z- vibration parameters of key components

The initial value in the horizontal /X- direction								
-0.3119	-0.2785	0.1023	0.1268	-0.1164	0.084	-0.069	-0.4229	-0.4643
-0.1478	-0.4684	-0.1081	0.1793	-0.3894	-0.4463	0.1126	0.1117	-0.4237
The value after training								
-7.044463	4.182612	-1.837496	2.487431	3.748632				

The trained network structure is used to test the fault sample data, and the results are shown in Tab. 5[5].

Table 5

Sample data

Inner ring fatigue (Sample 1)	0.1464	0.1443	0.9836	0.0000	0.0000	0.0124
Inner ring fracture (Sample 2)	0.0021	0.9964	0.1382	0.0000	0.0009	0.0000
Outer ring fatigue (Sample 3)	0.0003	0.1469	0.0004	0.9894	0.0000	0.0049
Outer ring fracture (Sample 4)	0.0860	0.0000	0.0002	0.9942	0.0007	0.0017

The output results in the above table are processed. The output matrix is taken, and the fault diagnosis mode is obtained. The diagnosis conclusion is drawn [18]. The diagnosis results of PARD-BP network are completely consistent in Tab. 6. It can be seen from the analysis that the PARD-BP network can identify different forms of faults and diagnose faults accurately [1].

Table 6

PARD-BP network diagnosis results

Sample number	Failure mode						Diagnostic conclusion
Sample 1	0	0	1	0	0	0	Inner ring fatigue
Sample 2	0	1	0	0	0	0	Inner ring fracture
Sample 3	0	0	0	1	0	0	Outer ring fatigue
Sample 4	0	0	0	1	0	0	Outer ring fracture

5. Result analysis

The static characteristics of the spindle system are shown in Table 7 below. Through the analysis of the spindle system, it is found that the stress of the spindle system is

mainly concentrated on the side rib plate and the inner rib plate, so it is important to optimize the size of the inner rib plate and the side rib plate.

Table7

Statics characteristic of the spindle system

Loading direction	Maximum deformation (μm)	Maximum stress (Pa)
X	11.7	880118
Y	1.51	118932
Z	1.34	125416

The structural diagram before and after the optimization of the spindle system is shown in Figure 5 in the dynamic test of the three-spindle machining center. The mechanical characteristics of the spindle system monomer after optimization are obtained by optimizing the inner and side ribs of the spindle system, and the mechanical characteristics of the spindle system monomer before and after optimization are compared, as shown in Tab. 8 [16].

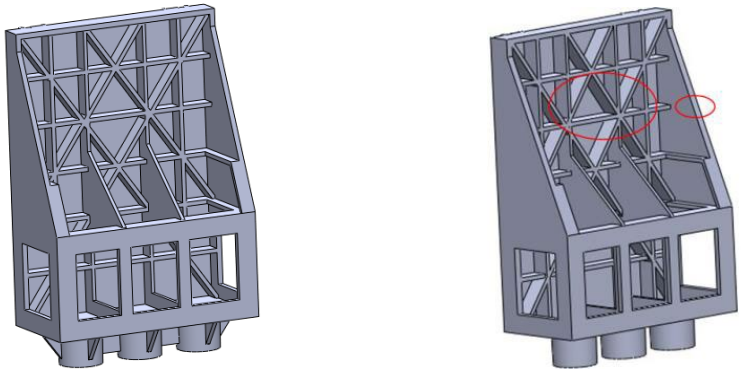

a) Before optimization b) After optimization

Fig.4 The optimization of the spindle system

Tab.8 **Mechanical properties before and after the optimization of the spindle system monomer**

	Direction	Maximum deformation(μm)	Maximum stress(Pa)	Mass (kg)
After optimization	X	10.7	805682	306.5 (Original mass: 297.5kg)
	Y	1.40	107689	
	Z	1.23	112853	
Rate of change	X	-8.54%	-9.24%	3.02%
	Y	-7.28%	-9.45%	
	Z	-8.94%	-10.02%	

The primary mass of spindle system is 297.5kg. By comparing the mechanical characteristics of the spindle system before and after the single factor optimization, it is found that the weight of the spindle system only increases by 3.02% after the single factor optimization, the mechanical characteristics of the spindle system are improved, and the three axial strains are all decreased, indicating

that the stiffness is increased, and the stress on the three axes is also reduced, especially the Z-axis, which is reduced by -10.02%. It indicates that the mechanical characteristics of the spindle system have been improved [19].

6. Summary

In this paper, the main shaft bearing of machining center dynamic element main shaft system is studied, and the algorithm theory and test data acquisition and comparison method are proposed. The algorithm and test method used in this paper are effective for fault monitoring and control and can further improve the control reliability and dynamic performance of the spindle system of the machining center, and improve the machining precision and efficiency of the spindle system. This method can provide technical reference for the fault diagnosis and dynamic performance stability of spindle systems of other types of multi-axis machine tools, rotating parts and other mechanical parts, and has important significance and application potential for the exploration of fault diagnosis and algorithm of related mechanical ontology and rotating parts in mechanical engineering and automotive engineering fields.

Acknowledgements

The research was supported by: 1. Anhui Quality Engineering Project: Electromechanical integration technology professional teaching team (2021jxtd072); 2. Anhui University Outstanding top talent cultivation program (gxbjZD2022149); 3. Special training for complex technical talents of industrial robot intelligent manufacturing professional group (WJ-ZYPX-099); 4. Anhui Quality Engineering Project: Anhui provincial "Three Education" reform demonstration school project (2022sjgg006); 5. Anhui Quality Engineering Project: Research platform for improving teaching ability of young teachers in higher vocational colleges (2022ptjs005); 6. High-level university teaching and research projects will create a technical skills innovation service platform; 7. 2021 Action Plan for Improving the quality of vocational education - The construction and application of shared professional teaching resources library; 8. 2021 Vocational Education Quality Improvement Action Plan provincial-level - promote the pilot of 1+X certificate system.

REFERENCES

[1] *Q. Zhou, L. Liu.* “Research on fault diagnosis of complex equipment based on artificial intelligence”, Journal of Physics: Conference Series, **vol.** 1550, no. 2, 2020, 022-028.

[2] *R. T. Zhang, B. B. Li, B. Jiao.* “Application of Xgboost algorithm in bearing fault diagnosis”, IOP Conference Series: Materials Science and Engineering, **vol.** 490, no. 7, 2019, 072062.

[3] *Y. S. Qi, C. Y. Guo, F. Shi, et al.* "Intelligent Fault Diagnosis of Rolling Bearing Based on Dual Structure Deep Learning", Vibration and Shock, **vol.** 40, no. 10, 2021, 103-113
[4] *X. L. Feng, G. Zhao, Y. Wang, D. J. Gao, H. Ding*. "Fault diagnosis method7 based on the multi-head attention focusing on data positional information", Measurement and Control, 2022
[5] *S. T. Xi, H. R. Cao, X. F. Chen, et al.* "Dynamic modeling of machine tool spindle bearing system and model based diagnosis of bearing fault caused by collision", Procedia CIRP, **vol.** 77, 2018, 614-617.
[6] *T. Berredjem, M. Benidir.* "Bearing faults diagnosis using fuzzy expert system relying on an improved range overlaps and Similarity method", Expert Systems with Applications, **vol.** 108, 2018, 134-142
[7] *W. D. Cheng, E. Z. Zhao, D. D. Liu.* "Fault diagnosis of rolling bearing with variable speed based on fault characteristic coefficient template", Vibration and shock, **vol.** 36, no. 7, 2017, 123-129.
[8] *N. N. Zhang, L. F. Wu, J. Yang, et al.* "Naive bayes bearing fault diagnosis based on enhanced independence of data", Sensors, **vol.** 18, no. 2, 2018, 463-468.
[9] *H. Li, H. Gao, H. Liu, et al.* "Fault-tolerant H control for active suspension vehicle systems with actuator faults", Proceedings of the Institution of Mechanical Engineers. Part I: Journal of Systems and Control Engineering, **vol.** 226, no. 3, 2012, 348-363.
[10] *Y. J. Qiang, L. Chen, L. Hua, J. P. Gu, L. J. Ding, Y. Q. Liu.* "Research on the Classification for Faults of Rolling Bearing Based on Multi-weights Neural Network", International Journal on Smart Sensing and Intelligent Systems, **vol.** 7, no. 3, 2014, 1004-1023.
[11] *J. Zhou, Q. Sun, W. Huang, Q. Zhang, C. Y. Shi.* "Two mechanical fault diagnosis algorithms based on the serial integration of CNN model", Journal of Army Engineering University, **vol.** 2, no. 02, 2023, 31-38.
[12] *Y. J. Li, Q. Liu, W. Li.* "Research and application of impeller fault intelligent diagnosis method based on digital twin flow field cloud map of centrifugal pump", Journal of Beijing University of Aeronautics and Astronautics, accepted, 10.13700/j.bh.1001-5965.2022.0997.
[13] *W. Huang, J. D. Zheng, J. Y. Tong, H. Y. Pan and Q. Y. Liu.* "Application of AM-FM Operator Decomposition Method in Rolling Bearing Fault Diagnosis", 10.13433/j.cnki.1003-8728.20230019
[14] *J. Zhou, Y. Gao, J. P. Lu, C. Yin, H. Han.* "An Ensemble Learning Algorithm for Machinery Fault Diagnosis Based on Convolutional Neural Network and Gradient Boosting Decision Tree", Journal of Physics: Conference Series, 2021.
[15] *J. An, P. Ai, D. K. Liu, et al.* "Deep domain adaptation model for bearing fault diagnosis with domain alignment and discriminative feature learning", Shock and Vibration, **vol.** 2020, 2020, 1-10.
[16] *X. Chen.* "Fault diagnosis of high power grid wind turbine based on particle swarm optimization BP neural network during COVID-19 epidemic period", Journal of Intelligent & Fuzzy Systems, **vol** 39, no. 6, 2020, 9027-9035.
[17] *C. Q. Shen, J. Q. Xie, D. Wang, et al.* "Improved hierarchical adaptive deep belief network for bearing fault diagnosis", Applied Sciences, **vol.** 9, no. 16, 2019, 3374.
[18] Communications, Signal Processing and Systems, Springer Science and Business. Media LLC, 2020.
[19] *H. Jiang, J. G. Yang, X. D. Yao, et al.* "Residual Correction of Thermal Error Model of a Bedroom Machining Center Based on BP Neural Network", Journal of Mechanical Engineering, no. 15, 2013, 115-121.